Procedure to Define an Accurate Model for Saturation and Cross-Coupling in IPM Machines

A. Di Gerlando, G. M. Foglia, R. Perini

***Abstract* -- IPM machines are characterized by high saturation and cross-coupling effect. In this paper a procedure is proposed to identify an IPM machine model able to taking into account in a simple and accurate manner both the cited effects. The model is based on functions that express the direct links $\bar{\psi}_{sdq}(\bar{i}_{sdq})$, and the inverse link $\bar{i}_{sdq}(\bar{\psi}_{sdq})$, where $\bar{i}_{sdq}$ and $\bar{\psi}_{sdq}$ are the stator current and stator flux linkage space vectors respectively. The paper shows that such a model is helpful for the analysis of both steady state and transient operation.**

***Index Terms*— space vector, saturation, cross coupling, FEM identification of flux linkage-current links, flux linkage-current space vectors links.**

I. Introduction

Usually in electrical machines models, the flux linkages–current relations are based on axis inductances L_d, L_q. For their geometrical structure, the IPM (Internal Permanent Magnet) machines are the most prone to high saturation, and great cross-coupling effects. Thus, axis inductances are not constant, but depend on currents, and both L_d, L_q depend on both currents i_d, i_q. This makes difficult the definition and the usage of functions $L_d(i_d, i_q)$, $L_q(i_d, i_q)$, especially if in the state equations the current is chosen as state variable. Therefore, several proposals can be found in literature about how defining inductance functions.

The most used approach is defining some "self and mutual axis inductance functions", given by the partial derivatives of the axis fluxes with respect to the axis currents: in particular, $L_{dd} = \partial\psi_d(i_d, i_q)/\partial i_d$, $L_{qq} = \partial\psi_q(i_d, i_q)/\partial i_q$, $L_{dq} = \partial\psi_d(i_d, i_q)/\partial i_q$, $L_{qd} = \partial\psi_q(i_d, i_q)/\partial i_d$ [1]-[3], [6], [8].

Such inductances are then multiplied by the axis current time derivatives, to get the flux linkages derivatives. Functions $\psi_d(i_d, i_q)$ and $\psi_q(i_d, i_q)$ can be identified by FEM [1]-[3], [5], [6], [8] or also by test measurements [1], [2]. The FEM or experimental data can be used as look-up tables, or can be used in fitting functions [1], [2], [5], [6], [8]. Anyway, often the formulation is not easy, and sometimes not clear.

An alternative approach is using the flux linkage as state variable: in this case, inductances are not needed, and the links $\bar{\psi}_{sdq}(\bar{i}_{sdq})$ and $\bar{i}_{sdq}(\bar{\psi}_{sdq})$ are used. This approach is little used in literature [5], [7].

In this paper, an approach similar to [7] is used; differently from to [7], here the aim is to outline in detail the procedure used to define the model; moreover, the model is applied to analyze both steady state and transient operating conditions.

The procedure starts with the definition of the direct link $\bar{\psi}_{sdq}(\bar{i}_{sdq})$, and of the inverse link $\bar{i}_{sdq}(\bar{\psi}_{sdq})$, where $\bar{i}_{sdq}$ and $\bar{\psi}_{sdq}$ are the stator current and stator flux linkage space vectors respectively. These links are obtained starting from a matrix of points (gained by FEM 2D simulations), which gives the flux linkages values for different values of the current, and for several rotor positions within one pole pair rotor rotation. Even if special attention must be paid in choosing the number of the FEM solution points, in principle FEM approach allows to account for saturation, cross coupling, and PM flux in a very precise manner.

Then, by suited interpolations, continuous functions $\bar{\psi}_{sdq}(\bar{i}_{sdq})$ are created. By using a zeroing procedure, a matrix follows which expresses the inverse link $\bar{i}_{sdq}(\bar{\psi}_{sdq})$; again, interpolations lead to obtain continuous functions.

A very important step is the identification of the correct definition domain of axis fluxes ψ_{sd} and ψ_{sq} , otherwise the extrapolation can give non sensible values; the matter is solved by defining a suited ellipse in the plane (ψ_{sd} , ψ_{sq}).

Inverse function $\bar{i}_{sdq}(\bar{\psi}_{sdq})$ allows using the flux linkage as state variable, so inductances are not needed, and the machine model usage is much simpler.

In the following, the cited steps are presented and described. Then, the use of the model is exemplified in two conditions: 1) evaluation of the MTPA (Maximum Torque Per Ampere) current angle, that is the angle of the current space vector, required for MTPA operation; 2) an example of transient operation with a load torque step variation. In both cases, the proposed model is validated by comparison with 2D FEM simulations (by Ansys Maxwell). Finally, a comparison with a simplified model neglecting cross coupling is carried out.

II. Considered IPM Machine

The analysis is applied to an 8-pole IPM machine, with V-shaped PMs. Due to inverter current limits, the machine is equipped with two three-phase windings: each of them is distributed along half the stator periphery; the two current terns are in phase. Table I reports the machine main data, where torque and power data refer to the whole machine.

Fig. 1 shows a one-pole motor cross section.

TABLE I
MAIN DATA OF THE CONSIDERED IPM MACHINE

Rated line-line voltage V_n [V_{rms}]	190
Rated current I_n [A_{rms}]; rated power P_n [kW]	376; 180
Rated torque T_n [Nm]; rated speed N_n [rpm]	324; 5300
Pole pair number n; PM type	4; SmCo
Phase resistance R_{ph} [mΩ]; rotor inertia [kgm^2]	16.82; 0.035

Lombardy Region Government, Italy, has partially funded the research with POR/FESR INPROVES grant (ID 241363).

A. Di Gerlando, G. M. Foglia and R. Perini are with Politecnico di Milano, Department of Energy, Italy, antonino.digerlando@polimi.it, gianmaria.foglia@polimi.it, roberto.perini@polimi.it.

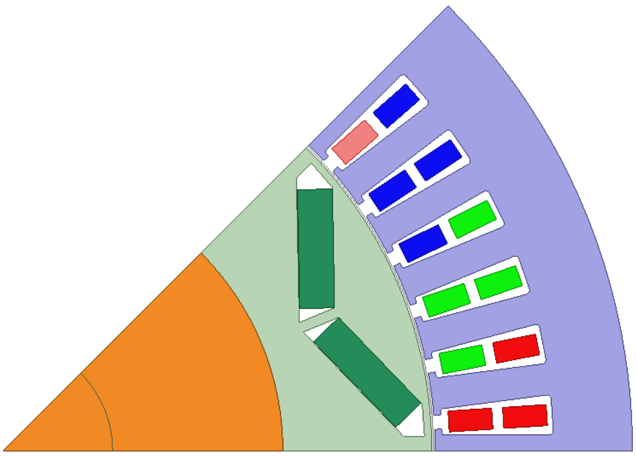

Fig. 1. One-pole cross section of the studied IPM machine.

As cited before, IPM motors are chosen here since saturation and cross-coupling effects are more apparent.

III. Evaluation of Direct Flux – Current Relations

Let us assume the conventions shown in Fig. 2: stator reference frame αβ, with α axis aligned with stator phase *A* axis; rotor reference frame *dq*, with *d* axis aligned with the PM axis; θ is the electrical angle between *d* and α; stator flux linkage space vector $\overline{\psi}_{sdq} = \psi_{sd} + j\cdot\psi_{sq} = \Psi_{sdq}\cdot\exp(j\cdot\varphi_\psi)$; stator current space vector $\overline{i}_{sdq} = i_{sd} + j\cdot i_{sq} = I_{sdq}\cdot\exp(j\cdot\varphi_I)$; both $\overline{\psi}_{sdq}$ and $\overline{i}_{sdq}$ are defined in *dq* reference frame.

The aim is to obtain the direct relations $\psi_{sd}(i_{sd}, i_{sq})$ and $\psi_{sq}(i_{sd}, i_{sq})$, which express $\overline{\psi}_{sdq}$ components as a function of $\overline{i}_{sdq}$ components.

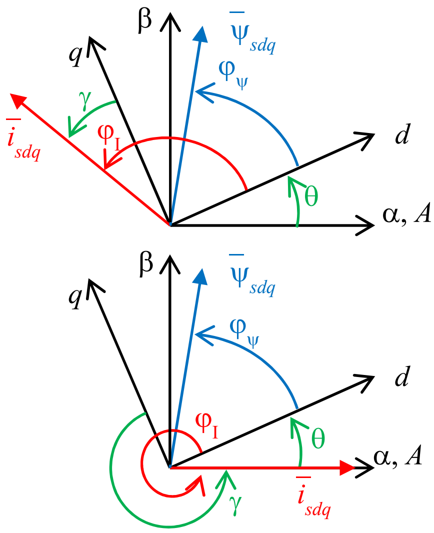

Fig.2. Stator reference frame αβ, rotor reference frame *dq*, current and flux space vectors; top: generic condition; bottom: condition chosen for FEM simulations, with frozen stator currents ($\overline{i}_{sdq}$ oriented along A phase axis).

To do so, we should set a rotor position, and move $\overline{i}_{sdq}$ to span a double polar pitch (360 electrical deg); each position corresponds to a couple (i_{sd}, i_{sq}), and for each couple the flux values ψ_{sd}, ψ_{sq} are evaluated. The same result is obtained if $\overline{i}_{sdq}$ is fixed in αβ reference frame, and the rotor is rotated. For the FEM simulations, the latter method is much simpler (because $\overline{i}_{sdq}$ fixed in αβ requires constant values of the phase currents): thus, several 2D FEM simulations are performed, where we set $\overline{i}_{sdq}$, and we consider k_{pos} rotor positions within a double polar pitch (i.e., θ assumes k_{pos} values θ_k between 0 and 360 electrical deg). This can be done either by using a magneto-static solver, and a script file which changes the rotor position, or by a transient solver, which moves the rotor. Vector $\overline{i}_{sdq}$ can be placed everywhere in αβ frame; a sensible choice is aligning it with α axis (Fig. 2 (bottom)), that is $\varphi_I = -\theta$, thus $\overline{i}_{sdq} = I_{sdq}\cdot\exp(-j\cdot\theta)$, or $i_{sd} = I_{sdq}\cdot\cos(-\theta)$, $i_{sq} = I_{sdq}\cdot\sin(-\theta)$. This choice does not correspond to any motor operating condition, but it is the simplest one for the FEM simulations.

Moreover, the instantaneous values of the phase currents equal $i_A = \sqrt{(2/3)}\cdot I_{sdq}$, $i_B = i_C = -i_A/2$.

For each rotor position θ_k, the FEM solver gives the stator phase flux linkages ψ_{sA}, ψ_{sB}, ψ_{sC}, and $\overline{\psi}_{sdq}$ is evaluated by applying the space vector definition

$$\overline{\psi}_{sdq} = \psi_{sd} + j\psi_{sq} = \sqrt{2/3}\cdot\{\psi_{sA} + \bar{a}\cdot\psi_{sB} + \bar{a}^2\cdot\psi_{sC}\}\cdot \cdot\exp(-j\cdot\theta), \qquad \bar{a} = \exp(j\,2\pi/3) \tag{1}$$

Thus, for one value I_{sdq} (magnitude of $\overline{i}_{sdq}$), ψ_{sd} and ψ_{sq} are expressed as a function of $\varphi_I = -\theta$ (phase of $\overline{i}_{sdq}$).

Actually, there is not a continuous function, but two vectors $[\psi_{sd}]$ and $[\psi_{sq}]$, with k_{pos} rows. To obtain a continuous function, FFT is performed on the vectors $[\psi_{sd}]$ and $[\psi_{sq}]$, that leads to the following Fourier development:

$$\psi_{sd}(\theta) = \textstyle\sum_h \Psi_{sdh} cos(h\theta),\ \psi_{sq}(\theta) = \sum_h \Psi_{sqh} sin(h\theta) \tag{2}$$

with $h = 1 \ldots h_{MAX}$ harmonic order, and Ψ_{sdh} , Ψ_{sqh} the FFT coefficients; do note that, thanks to the machine symmetry, $\psi_{sd}(\theta)$ has only cosine terms, and $\psi_{sq}(\theta)$ only sine terms.

Now, the procedure is repeated for k_I values of I_{sdq}, between 0 and the maximum current I_{sdq_max} (here equal to 1000 A). Thus, we obtain 3 vectors with k_I rows: a current vector $[I_{sdq}]$ and two function vectors $[\psi_{sd}(\theta)]$ and $[\psi_{sq}(\theta)]$, each row corresponding to one I_{sdq} value. Actually, the function vectors $[\psi_{sd}(\theta)]$ and $[\psi_{sq}(\theta)]$ are represented by the corresponding FFT coefficient vectors; thus, we have h_{MAX} vectors $[\Psi_{sdh}]$, and h_{MAX} vectors $[\Psi_{sqh}]$ (one vector for each harmonic; each vector has k_I rows, one row for each I_{sdq} value). To obtain a continuous function of the current, an interpolation on the FFT coefficients vectors is applied; in particular, for each harmonic *h*, a continuous function is obtained by interpolating $[\Psi_{sdh}]$, $[\Psi_{sqh}]$, with respect to $[I_{sdq}]$:

$$\psi_{sdh}(I_{sdq}) = interp([\Psi_{sdh}],[I_{sdq}])\ ,$$

$$\psi_{sqh}(I_{sdq}) = interp([\Psi_{sqh}],[I_{sdq}]) \tag{3}$$

These functions replace the FFT coefficients Ψ_{sdh} , Ψ_{sqh} in (2). Moreover, the relation $\varphi_I = -\theta$ is applied. Thus, the fluxes ψ_{sd} and ψ_{sq} are obtained as continuous functions of both I_{sdq} and φ_I (magnitude and phase of $\overline{i}_{sdq}$):

$$\psi_{sd}(I_{sdq},\varphi_I) = \textstyle\sum_h \psi_{sdh}(I_{sdq})\cdot cos(-h\cdot\varphi_I) \qquad ,$$

$$\psi_{sq}(I_{sdq},\varphi_I) = \textstyle\sum_h \psi_{sqh}(I_{sdq})\cdot sin(-h\cdot\varphi_I) \tag{4}$$

Some examples of $\psi_{sd}(I_{sdq},\theta)$, $\psi_{sq}(I_{sdq},\theta)$, are shown in Fig. 3.

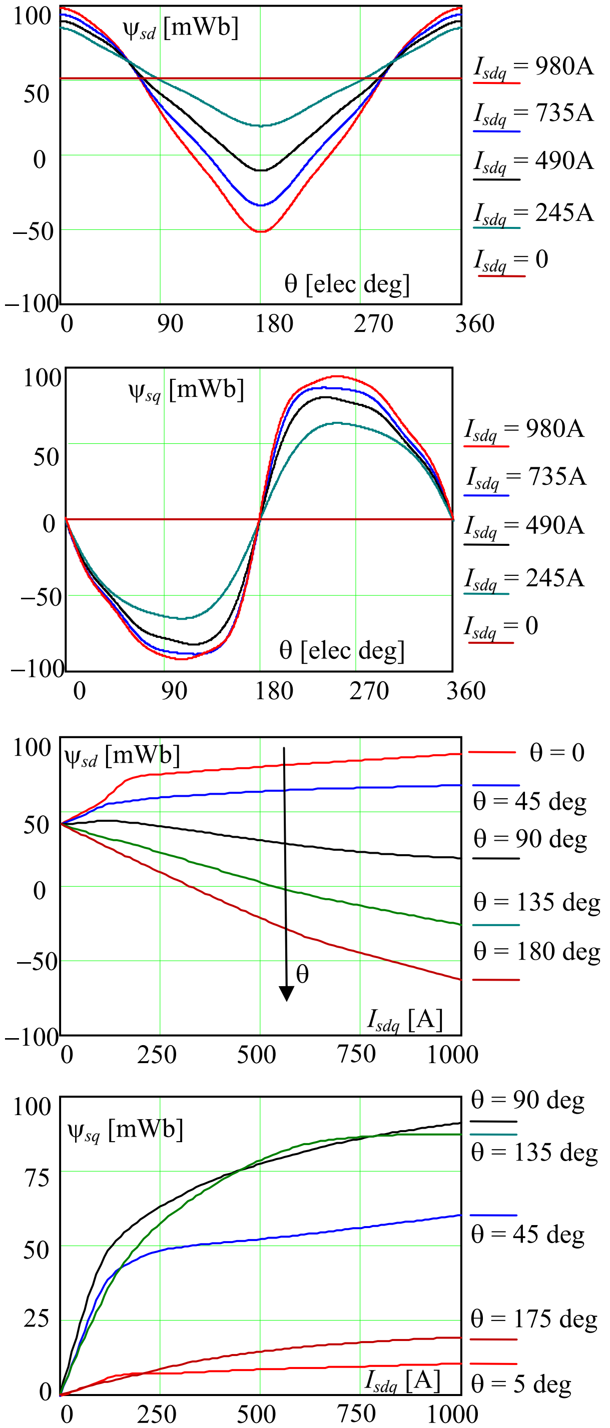

Fig.3. Examples of functions $\psi_{sd}(I_{sdq}, \theta)$, $\psi_{sq}(I_{sdq}, \theta)$.

Considering the relations between I_{sdq}, φ_I and i_{sd}, i_{sq}

$$I_{sdq} = \sqrt{{i_{sd}}^2 + {i_{sq}}^2} \quad \varphi_I = atan(i_{sq}/i_{sd}) \tag{5}$$

ψ_{sd} and ψ_{sq} are expressed as continuous functions of i_{sd}, i_{sq} :

$$\psi_{sd}(i_{sd}, i_{sq}) =$$

$$= \sum_{h=1}^{h_{MAX}} \psi_{sdh}\left(\sqrt{{i_{sd}}^2 + {i_{sq}}^2}\right) \cdot cos\left(-h \cdot atan\left(\frac{i_{sq}}{i_{sd}}\right)\right)$$

$$\psi_{sq}(i_{sd}, i_{sq}) = \sum_{h=1}^{h=h_{MAX}} \psi_{sqh}\left(\sqrt{{i_{sd}}^2 + {i_{sq}}^2}\right) \cdot$$

$$\cdot\, sin\left(-h \cdot atan(i_{sq}/i_{sd})\right) \tag{6}$$

Thus, the space vector of the stator flux linkages $\overline{\psi}_{sdq}$ is completely defined, as a function either of I_{sdq} , φ_I or i_{sd}, i_{sq} .

$$\overline{\Psi_{sdq}}(I_{sdq}, \varphi_I) = \psi_{sd}(I_{sdq}, \varphi_I) + j \cdot \psi_{sq}(I_{sdq}, \varphi_I) \tag{7}$$

$$\overline{\Psi_{sdq}}(i_{sd}, i_{sq}) = \psi_{sd}(i_{sd}, i_{sq}) + j \cdot \psi_{sq}(i_{sd}, i_{sq}) \tag{8}$$

As concerns the values of k_{pos}, k_I, h_{MAX}, the following remarks hold:

- k_{pos} should be rather high, to allow a good reconstruction of the flux-angle relation; we adopted $k_{pos} = 1080$;
- k_I cannot be too low, otherwise a wrong flux-current relation is obtained; we adopted $k_I = 40$;
- as regards the maximum order h_{MAX}, we assumed $h_{MAX} = 7$, in order to filter the tooth harmonics effect. An example of the amplitude of such harmonics is shown later, in Fig. 5.

IV. Evaluation of Inverse Current-Flux Relations

In order to adopt the flux as a state variable, the inverse relations which express i_{sd}, i_{sq} as a function of ψ_{sd}, ψ_{sq} are needed. For a couple of values $\psi_{sd}{}^*$, $\psi_{sq}{}^*$, the corresponding values $i_{sd}{}^*$, $i_{sq}{}^*$ can be found by solving numerically the system (6); thus, $i_{sd}{}^*$, $i_{sq}{}^*$ are the solutions of the system:

$$\begin{cases} \psi_{sd}(i_{sd}{}^*, i_{sq}{}^*) = \psi_{sd}{}^* \\ \psi_{sq}(i_{sd}{}^*, i_{sq}{}^*) = \psi_{sq}{}^* \end{cases} \tag{9}$$

By solving (9) for some values of ψ_{sd} and ψ_{sq}, corresponding i_{sd}, i_{sq} values of the relations $i_{sd}(\psi_{sd}, \psi_{sq})$, $i_{sq}(\psi_{sd}, \psi_{sq})$ follow. In particular, N_d values of ψ_{sd} and N_q values of ψ_{sq} are chosen, equally spread between maximum and minimum values of ψ_{sd} and ψ_{sq} ; for instance, Fig. 3 shows that the ranges are about -50 mWb $< \psi_{sd} <$ 100 mWb, -100 mWb $< \psi_{sq} <$ 100 mWb. Thus, two vectors are obtained, $[\psi_{sd\_i}]$ of N_d rows, $[\psi_{sq\_i}]$ of N_q rows (footer "*i*" stands for "inverse function"). By solving (9) for all the values of vectors $[\psi_{sd\_i}]$, $[\psi_{sq\_i}]$, two matrices are obtained, $[i_{sd\_i}]$, $[i_{sq\_i}]$, both with N_d rows and N_q columns; each element (j,k) satisfies system (9):

$$\begin{cases} \psi_{sd}\left([i_{sd\_i}]_{j,k}, [i_{sq\_i}]_{j,k}\right) = [\psi_{sd}]_j \\ \psi_{sq}\left([i_{sd\_i}]_{j,k}, [i_{sq\_i}]_{j,k}\right) = [\psi_{sq}]_k \end{cases} \quad \begin{cases} j = 1..N_d \\ k = 1..N_q \end{cases} \tag{10}$$

Next step is to move from matrixes $[i_{sd\_i}]$,$[i_{sq\_i}]$ to continuous functions $i_{sd}(\psi_{sd}, \psi_{sq})$, $i_{sq}(\psi_{sd}, \psi_{sq})$. To do so, a double interpolation of matrixes $[i_{sd\_i}]$,$[i_{sq\_i}]$ is performed: first, each of the N_q columns $[i_{sd\_i}]_{col\_k}$,$[i_{sq\_i}]_{col\_k}$ (each column has N_d rows) are interpolated with $[\psi_{sd\_i}]$ (which has N_d rows); we obtain N_q interpolating functions; thereafter, these N_q functions are interpolated with $[\psi_{sq\_i}]$ (which has N_q rows).

$$i_{sd_{interp}}(\psi_{sd}, \psi_{sq}) =$$

$$= interp\left(interp\left([i_{sd\_i}]_{col\_k}, [\psi_{sd\_i}]\right), [\psi_{sq\_i}]\right)$$

$$i_{sq_{interp}}\left(\psi_{sd},\psi_{sq}\right) =$$
$$= interp\left(interp\left(\left[i_{sq\_i}\right]_{col\_k},\left[\psi_{sd\_i}\right]\right),\left[\psi_{sq\_i}\right]\right) \quad (11)$$

V. Definition of the Correct Flux Ranges

In functions (4), the $\bar{i}_{sdq}$ domain is $0 < I_{sdq} < I_{sdq\_max}$, $0 < \varphi_I < 2\pi$: in (i_{sd}, i_{sq}) plane, the current limiting line is a circumference with radius equal to I_{sdq_max} . In (ψ_{sq} , ψ_{sd}) plane, the corresponding limiting flux contour is obtained by plotting functions (4) in a polar plot, at the maximum current I_{sdq_max} ; a line with a rough elliptic shape is found (black continuous line in Fig. 4). Points outside this rough elliptic line correspond to values of current outside the definition domain. This implies that the currents i_{sd}^*, i_{sq}^* found by (9) are meaningful only if the fluxes ψ_{sd}^*, ψ_{sq}^* are inside the cited rough elliptic line.

In (11), the domain of definition is a rectangle with $\psi_{sd\_min} < \psi_{sd} < \psi_{sd\_max}$, $\psi_{sq\_min} < \psi_{sq} < \psi_{sq\_max}$ (green lines in Fig. 4). The corners of this rectangle are outside the rough elliptic contour, therefore the definition domain of (11) is not correct; indeed, (11) do not work well (some current values get very high). A correction must be introduced in (11), to make the fluxes stay inside the rough elliptic line.

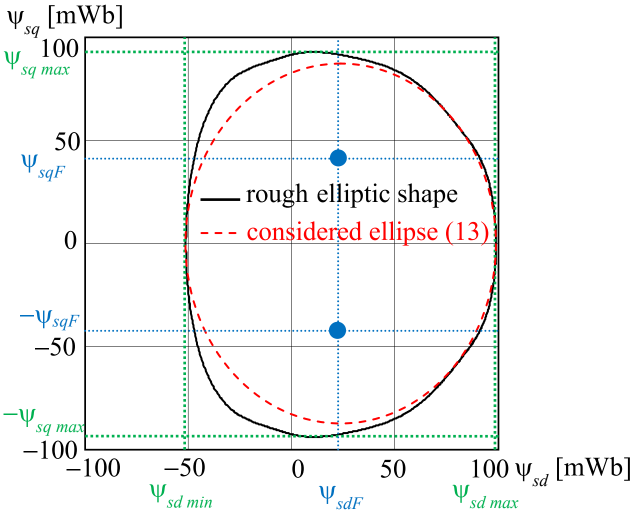

Fig. 4. Original elliptic shape, corresponding to polar plot of (4), and ellipse considered in (13).

First, the rough elliptic contour is substituted by an ellipse (red dotted line in Fig. 4) which is as much as possible similar to the rough elliptic contour, and completely inside it. By means of geometrical relations, both the foci coordinates (ψ_{sdF} , $\pm\psi_{sqF}$) and the ellipse characteristic constant FD (Foci Distance, i.e. the sum of the distances from the ellipse foci) can be expressed as a function of the flux limiting values (ψ_{sd_min} , ψ_{sd_max} , ψ_{sq_min} , ψ_{sq_max}, with $|\psi_{sq\_min}| = |\psi_{sq\_max}|$).

Then, the sum of the distances of a generic point (ψ_{sd} , ψ_{sq}) from the foci (ψ_{sdF} , $-\psi_{sqF}$) and (ψ_{sdF} , ψ_{sqF}) equals

$$fd(\psi_{sd},\psi_{sq}) = \sqrt{(\psi_{sd}-\psi_{sdF})^2+\left(\psi_{sq}-\psi_{sqF}\right)^2} +$$
$$+\sqrt{(\psi_{sd}-\psi_{sdF})^2+\left(\psi_{sq}+\psi_{sqF}\right)^2} \quad (12)$$

and the condition to make the fluxes stay inside the ellipse is simply $fd(\psi_{sd}, \psi_{sq}) < FD = 2\cdot\psi_{sq\_max}$.

Thus, (11) changes in (13): a zero current value is forced in case of flux values outside the correct definition domain:

$$\mathrm{i}_{sd}\left(\psi_{sd},\psi_{sq}\right) =$$
$$= if\left[fd(\psi_{sd},\psi_{sq}) < FD, \mathrm{i}_{sd\_interp}\left(\psi_{sd},\psi_{sq}\right),0\right]$$
$$\mathrm{i}_{sq}\left(\psi_{sd},\psi_{sq}\right) =$$
$$= if\left[fd(\psi_{sd},\psi_{sq}) < FD, \mathrm{i}_{sq\_interp}\left(\psi_{sd},\psi_{sq}\right),0\right] \quad (13)$$

By considering the space vectors, the inverse relations current-flux can be defined as

$$\overline{\iota_{inv}}\left(\overline{\psi}_{sdq}\right) = i_{sd}\left(Re\left(\overline{\psi}_{sdq}\right), Im\left(\overline{\psi}_{sdq}\right)\right)$$
$$+j\, i_{sq}\left(Re(\overline{\psi}_{sdq}), Im(\overline{\psi}_{sdq})\right) \quad (14)$$

VI. Model Summary and Torque Expression

At the end, the model is based just on some interpolating functions, and some vectors or matrices:

- the direct relations flux – current (4) are obtained by means of interpolating functions (3), based on vectors [Ψ_{sdh}], [Ψ_{sqh}], [I_{sdq}] (gained by processing the data of some FEM simulations);
- the inverse relations current – flux (13) are obtained by means of interpolating functions (11), based on matrices [i_{sd_i}],[i_{sq_i}] (gained by numerical solution of system (9)).

Both the FEM simulations and the numerical solution of system (9) are performed just once, in order to get the vectors or matrices needed for the interpolation. Afterwards, the model just requires a software able to perform the interpolations (in our application, we adopted Mathcad 11).

The electromagnetic torque T_e has the classical expression:

$$T_e = -2 \cdot n \cdot Im(\ \overline{\psi}_{sdq}\ \underline{i}_{sdq}\ ), \quad (15)$$

where 2 is due to the two three-phase windings, n is the pole-pair number, $Im()$ is the Imaginary part operator, $\underline{i}_{sdq}$ is the conjugate of $\bar{i}_{sdq}$.

$\overline{\psi}_{sdq}$ (and, thus, T_e too) can be expressed as a function of either i_{sd} and i_{sq} or I_{sdq} and φ_I, by means of (8) or (7) respectively.

VII. Evaluation of the Current Angle for MTPA

If T_e is expressed as a function of I_{sdq} and φ_I, the current angle φ_{I_MTPA}, which gives the MTPA condition, can be obtained by performing a numerical derivative of the function $T_e(I_{sdq}$, φ_I) with respect to φ_I , and by zeroing such derivative. In such calculation, some troubles may occur, because φ_{I_MTPA} is higher than 90 deg; the matter is solved by substituting φ_I with γ + 90deg (see Fig. 2), and performing the same operation by using angle γ. As a result, the proposed model gives angle γ_{MTPA_mod} (which gives the MTPA condition), as a function of I_{sdq} (magnitude of $\bar{i}_{sdq}$):

$$T_e(I_{sdq},\varphi_I) = -2n \cdot Im\{\overline{\Psi_{sdq}}(I_{sdq},\varphi_I) \cdot I_{sdq} \cdot e^{-j\varphi_I}\} \quad (16)$$

$$T_e(I_{sdq},\gamma) = -2 \cdot n \cdot Im\{\overline{\Psi_{sdq}}(I_{sdq},\gamma + {}^{\pi}/_{2}) \cdot [I_{sdq} \cdot \exp(-j(\gamma + {}^{\pi}/_{2}))]\} \quad (17)$$

$$\frac{\Delta T_e(I_{sdq},\gamma)}{\Delta\gamma} = \frac{T_e(I_{sdq},\gamma+\Delta\gamma) - T_e(I_{sdq},\gamma)}{\Delta\gamma} \quad (18)$$

$$\gamma_{MTPA\_mod}(I_{sdq}) = zeroing\left[\frac{\Delta T_e(I_{sdq},\gamma)}{\Delta\gamma},\gamma\right] \quad (19)$$

In order to validate this procedure, the angle γ_{MTPA} has been found also by FEM simulations. In particular, the same solutions (with fixed current and moving rotor), which gave the flux linkages, also gave the holding torque (which is defined just as the torque with fixed current and moving rotor): therefore, for each of the k_I current values, we have a vector $[HT_{kI}]$, of k_{pos} holding torque values. In principle, $[HT_{kI}]$ can be transformed in a continuous function $HT_{kI}(\theta)$ of the rotor position θ, by means of an spline function; then, $HT_{kI}(\theta)$ can be derived, to gain the θ_{MTPA} value which maximizes the torque. Actually, the procedure is not so straightforward, due to stator slotting and harmonic MMFs, which cause a ripple in the holding torque. Thus, before derivation, function $HT_{kI}(\theta)$ is to be filtered to eliminate tooth harmonics; a simple way is performing a Fourier development of $HT_{kI}(\theta)$, and reconstructing the function just with the low order harmonics. Fig. 5 shows an example of $HT_{kI}(\theta)$ function, and the corresponding filtered function $HT_{kI\_filt}(\theta)$, for I_{sdq} = 602A.

According to Fig.2(b), the θ - γ relation is $\gamma + \theta = \pi \cdot 3/2$. Thus, γ_{MTPA_mod} can be found by differentiating $HT_{kI\_filt}(\pi \cdot 3/2 - \gamma)$ with respect to γ, and by zeroing the derivative.

Fig. 6 shows the comparison between $\gamma_{MTPA\_mod}(I_{sdq})$ and γ_{MTPA_FEM} : the good agreement validates the proposed model.

VIII. Analysis of Steady State operation in MTPA

In MTPA operation, angle γ value is obtained by (19). Therefore, given a desired torque value T_e*, the required current space vector $I_{sdq}{}^*\cdot\exp[\,j\,(\gamma_{MTPA}{}^* + \pi/2)\,]$ is obtained by (19) and (17):

$$T_e(I_{sdq}{}^*,\gamma_{MTPA}{}^*) = T_e^* \,,\gamma_{MTPA}{}^* = \gamma_{MTPA\_mod}(I_{sdq}{}^*) \quad (20)$$

By solving numerically (20), the required value I_{sdq}* and γ_{MTPA}* are obtained. Then, the required voltage space vector $V_{sdq}{}^*\cdot\exp[\,j\,\varphi_V{}^*\,]$ is gained by the voltage law:

$$V_{sdq}{}^* \cdot exp(j\,\varphi_V{}^*) = R_{ph} \cdot I_{sdq}{}^*\exp(j\,(\gamma_{MTPA}{}^* + \pi/2)) + j\,\omega\,\overline{\Psi_{sdq}}(I_{sdq}{}^*,\gamma_{MTPA}{}^* + \pi/2) \quad (21)$$

where ω is the angular frequency ($\omega = n\,2\pi N/60$; N [rpm] = speed, n = pole pair).

For instance, an operating point in MTPA is as follows:

$$N_{op} = 5000 \text{ rpm}; \quad T_{e.op} = 260 \text{ Nm:}$$
$$I_{sdq.op} = 504.9 \text{ A}; \ \gamma_{MTPA.op} = 46.4 \text{ deg} \quad (22)$$
$$V_{sdq.op} = 172.8 \text{ V}; \quad \varphi_{V.op} = 170.4 \text{ deg}$$

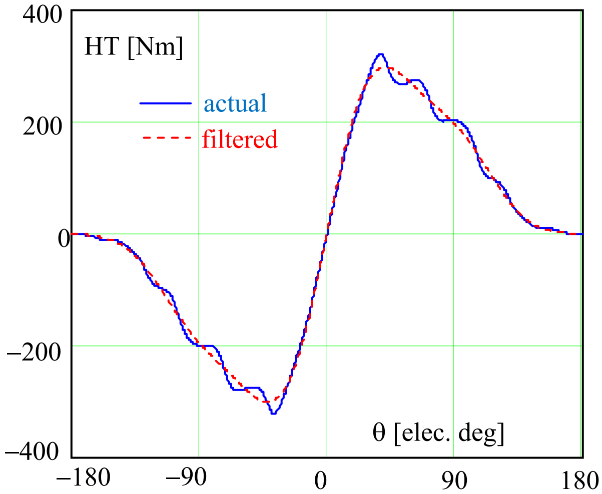

Fig.5. Holding torque as a function of the electrical angle. Continuous line: actual values, with ripple due to stator slotting. Dotted line: filtered function.

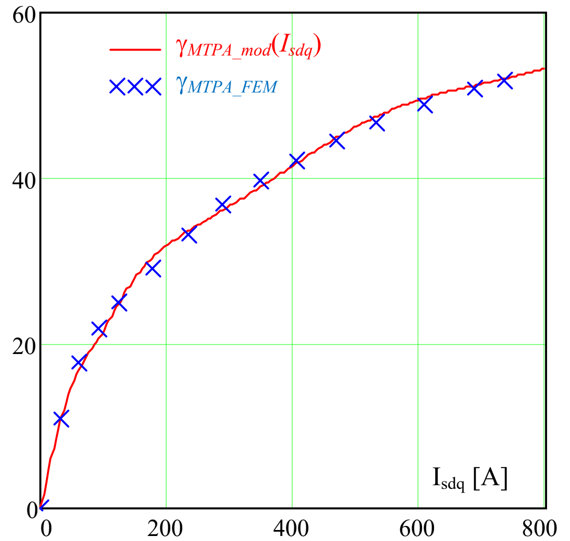

Fig. 6. Current angle γ_{MTPA} which gives maximum torque per ampere condition (MTPA), as a function of I_{sdq} (magnitude of current space vector); comparison between the angles evaluated by the proposed model ($\gamma_{MTPA\_mod}(I_{sdq})$) and by FEM simulations (γ_{MTPA_FEM}).

IX. Example of Transient Operation

In order to validate the proposed model in transient operation, a simple electromechanical transient has been simulated, and compared with a FEM solution. Since the aim is the flux-current link, and not the system stability, an open loop operation is considered, without any control system. In particular, a three-phase sinusoidal supply voltage (with constant rms phase voltage V_{sph} and constant angular frequency ω) is assumed and, starting from a steady state operation, a step variation of a fluid-dynamic load torque (i.e.: torque ∝ speed squared) has been applied.

The phase A voltage expression is $v_A(t) = \sqrt{2}\cdot V_{sph}\cdot\cos(\theta_V)$, where $\theta_V = \omega\cdot t + \theta_{V0}$. The phase voltage space vector in dq reference frame $\bar{v}_{sdq}$ can be expressed as:

$$\bar{v}_{sdq} = V_{sdq} \cdot \exp(j\,\varphi_V) = \sqrt{2/3}\,(\sqrt{2}V_{sph})[cos(\theta_V) + \bar{a} \cdot cos(\theta_V - 2\pi/3) + \bar{a}^2 \cdot cos(\theta_V - 4\pi/3)] \cdot \exp(-j\theta) \quad (23)$$

where φ_V is the phase with respect to d axis, θ_V is the phase with respect to real axis α, θ is the angle between d axis and real axis α (Fig. 7(a)); $\bar{a} = \exp(j\,2\pi/3)$; $V_{sdq} = \sqrt{3}\,V_{sph}$. It is assumed that $t = 0$ occurs when d axis is aligned to real axis α (Fig. 7 b), thus $\theta_{V0} = \varphi_{V0}$; moreover, it is assumed that in $t = 0$ the system is at steady state at operating point (22); thus, $\varphi_{V0} = \varphi_{V.op}$, $\omega = \omega_{op}$, $V_{sdq} = V_{sdq.op\_}$. Thus, $\bar{v}_{sdq}$ depends on time t and on d axis position θ, and $\bar{v}_{sdq}$ becomes:

$$\bar{v}_{sdq}(t,\theta) = \sqrt{2/3}\left(\sqrt{2/3}\,V_{sdq.op}\right)\left[\cos\left(\omega_{op}t+\varphi_{V.op}\right) + \bar{a}\cdot\cos\left(\omega_{op}t+\varphi_{V.op}-2\pi/3\right)+\bar{a}^2\cdot\cos\left(\omega_{op}t+\varphi_{V.op}-4\pi/3\right)\right]\cdot\exp(-j\theta) \quad (24)$$

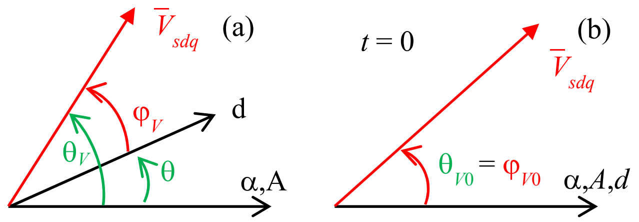

Fig.7. Phase voltage space vector. (a): generic position. (b): initial condition for the transient operation.

It is assumed that the fluid-dynamic load torque T_L starts from the steady state value (22) and, after a time interval Δt_{TL}, decreases by 10%. Thus, T_L depends on the time and on the angular frequency ω, and its expression can be written as:

$$T_L(t,\omega) = if\left[t < \Delta t_{TL}, T_{op}, 0.9\cdot T_{op}\cdot(\omega/\omega_n)^2\right] \qquad (25)$$

with ω_n rated angular frequency (ω_n=$2\pi n\cdot N_n$ /60 =2220rad/s). The state variables are θ, ω, and the stator flux linkage space vector $\bar{\psi}_{sdq}$; the current space vector is obtained by the inverse function (14); the state equations of the machine are:

$$\begin{aligned} \frac{d\theta}{dt} &= \omega \\ \frac{J_t}{n}\frac{d\omega}{dt} &= -n\cdot Im\left\{\bar{\psi}_{sdq}\cdot \overline{i_{inv}\left(\bar{\psi}_{sdq}\right)}\right\} - T_L(t,\omega) \qquad (26) \\ \frac{d\bar{\psi}_{sdq}}{dt} &= \bar{v}_{sdq}(t,\theta) - R_{ph}\cdot \overline{i_{inv}}\left(\bar{\psi}_{sdq}\right) - j\,\omega\,\bar{\psi}_{sdq} \end{aligned}$$

System (26) is integrated by backward Euler method, with a time step of 50 μs. As concerns the FEM simulation, the same transient was implemented in Ansys Maxwell, by means of a 2D transient simulation; the machine model is the one shown in Fig. 1, and a master-slave boundary condition has been used.

Fig.s 8 (a) and (b) show the comparison between the model results and the FEM results as concerns the electromagnetic torque T_e and the mechanical speed N.

It should be observed that the original FEM electromagnetic torque waveform (actual points) is affected by significant torque ripple (as shown in Fig. 5): it can be eliminated by filtering the original waveform by moving average.

The agreement is fair, and considering that the model simulation takes a few minutes, whereas the FEM simulation takes a few days, the proposed model can be considered a useful tool, especially for machine design and operation analysis.

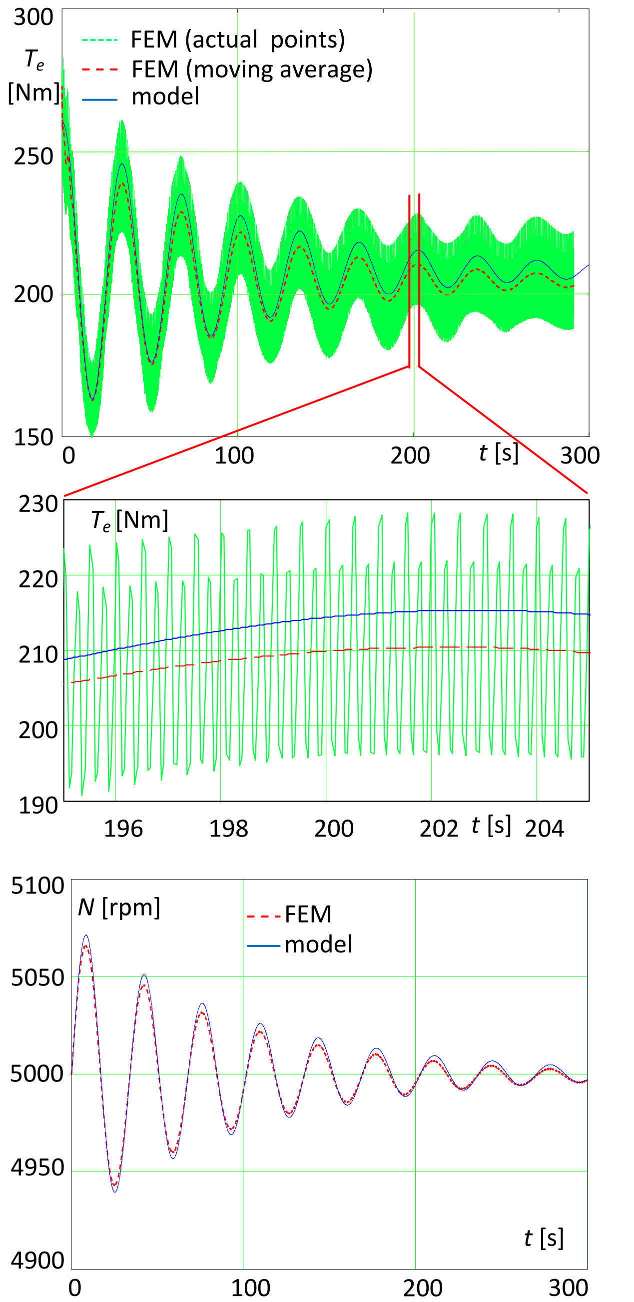

Fig. 8. Comparison between the model results and FEM results as concerns electromagnetic torque T_e (top) and mechanical speed N (bottom).

X. Example of Comparison with a Simplified Model

Once the proposed model has been validated, a comparison is carried out with the torque obtained by a simplified model, which assumes ψ_{sd} dependent only on i_{sd} and ψ_{sq} dependent only on i_{sq} (no cross coupling: subscript NOcc). Thus, two new functions ψ_{sd_NOcc} and ψ_{sq_NOcc} are defined. They can be obtained starting from (4), by expressing i_{sd} , i_{sq} as a function of I_{sdq} , φ_I . In particular, amplitude and phase of i_{sd} , i_{sq} can be expressed as

$$|i_{sd}| = |\,I_{sdq}\cdot\cos(\varphi_I)|\,,\ \ arg(i_{sd}) = if(-\pi/2 < \varphi_I < \pi/2;\,0;\,\pi)$$
$$|i_{sq}| = |\,I_{sdq}\cdot\sin(\varphi_I)|\,,\ \ arg(i_{sq}) = if(0 < \varphi_I < \pi;\,\pi/2;\,-\pi/2)$$

Inserting these quantities in (4) yields

$$\psi_{sd\_NOcc}\,(I_{sdq}\,,\varphi_I) =$$
$$\psi_{sd}\,(\,|\,I_{sdq}\cdot\cos(\varphi_I)|\,,\ \mathit{if}\,(\,-\pi/2<\varphi_I<\pi/2;\,0;\,\pi)\,)$$
$$\psi_{sq\_NOcc}\,(I_{sdq}\,,\varphi_I) = \tag{27}$$
$$\psi_{sq}\,(\,|\,I_{sdq}\cdot\sin(\varphi_I)|\,,\ \mathit{if}\,(\,0<\varphi_I\ <\pi;\,\pi/2;\,-\pi/2)\,)$$

By means of (27), flux linkage and torque of the model without cross coupling can be expressed simply as

$$\overline{\psi}_{sdq\_NOcc}(I_{sdq}\,,\varphi_I) = \psi_{sd\_NOcc}(I_{sdq}\,,\varphi_I) + j\ \psi_{sq\_NOcc}(I_{sdq}\,,\varphi_I) \tag{28}$$

$$T_{e\_NOcc} = -\,2\cdot n\cdot Im(\ \overline{\psi}_{sdq\_NOcc}\ \underline{i}_{sdq}\ ) \tag{29}$$

Fig. 9 shows, for three values of I_{sdq}, the torque as a function of φ_I, considering the proposed model (15) (continuous line) and the simplified model (29) (dotted line). It is apparent that the simplified model works well just for low currents, but it works worse and worse as saturation increases.

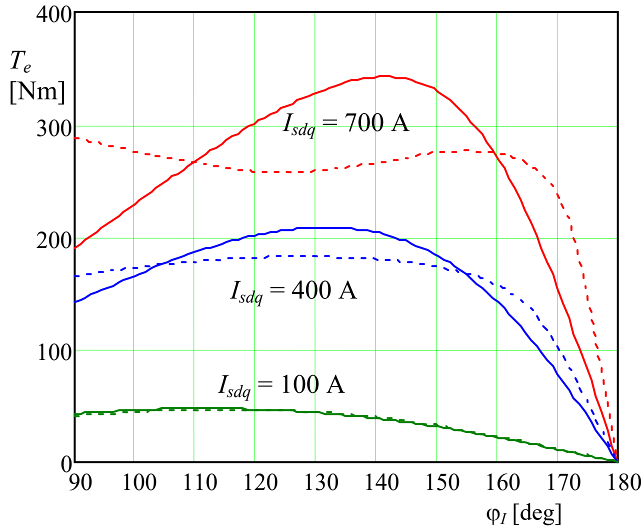

Fig. 9. Torque as a function of φ_I for three values of I_{sdq}, for the proposed model (15) (continuous line) and the simplified model (29) (dotted line).

XI. Conclusion

The paper deals with an IPM machine model able to taking into account both saturation and cross coupling effects accurately. The model does not use inductances, but the direct link flux linkage - current and the inverse link current - flux linkage, in terms of space vectors: the procedure adopted to define the cited links is described in detail.

The model has been validated by means of 2D FEM simulations, both for operation in steady state and in transient operating conditions. The model simulation time is greatly reduced compared with FEM simulation time, thus representing a useful tool for design and operation analysis.

If the torque is evaluated by a simplified model which does not take into account cross coupling, a great error occurs at high currents.

XII. References

[1] B. Stumberger, G. Stumberger, D. Dolinar, A. Hamler and M. Trlep, "Evaluation of saturation and cross-magnetization effects in interior permanent-magnet synchronous motor," in *IEEE Transactions on Industry Applications*, vol. 39, no. 5, pp. 1264-1271, Sept.-Oct. 2003. doi: 10.1109/TIA.2003.816538.

[2] Y. Li, Z. Q. Zhu, D. Howe and C. M. Bingham, "Modeling of Cross-Coupling Magnetic Saturation in Signal-Injection-Based Sensorless Control of Permanent-Magnet Brushless AC Motors," in *IEEE Transactions on Magnetics*, vol. 43, no. 6, pp. 2552-2554, June 2007. doi: 10.1109/TMAG.2007.892319.

[3] Z. Q. Zhu, Y. Li, D. Howe, C. M. Bingham and D. Stone, "Influence of Machine Topology and Cross-Coupling Magnetic Saturation on Rotor Position Estimation Accuracy in Extended Back-EMF Based Sensorless PM Brushless AC Drives," 2007 *IEEE Industry Applications Annual Meeting*, New Orleans, LA, 2007, pp. 2378-2385. doi: 10.1109/07IAS.2007.359.

[4] A. Wang, H. Li and C. Liu, "Assessments of magnetic cross-coupling impacts on interior permanent magnet machine controls for electric vehicles," 2009 *International Conference on Power Electronics and Drive Systems (PEDS)*, Taipei, 2009, pp. 1435-1438. doi: 10.1109/PEDS.2009.5385821.

[5] H. Nagura, Y. Iwaji, J. Nakatsugawa and N. Iwasaki, "New vector controller for PM motors which modeled the cross-coupling magnetic flux saturation," The 2010 *International Power Electronics Conference - ECCE ASIA -*, Sapporo, 2010, pp. 1064-1070. doi: 10.1109/IPEC.2010.5542095

[6] Z. Li and H. Li, "MTPA control of PMSM system considering saturation and cross-coupling," 2012 15th *International Conference on Electrical Machines and Systems* (ICEMS), Sapporo, 2012, pp. 1-5.

[7] R. Bojoi, A. Cavagnino, M. Cossale and S. Vaschetto, "Methodology for the IPM motor magnetic model computation based on finite element analysis," IECON 2014 - 40th *Annual Conference of the IEEE Industrial Electronics Society*, Dallas, TX, 2014, pp. 722-728. doi: 10.1109/IECON.2014.7048580

[8] A. Rabiei, T. Thiringer, M. Alatalo and E. A. Grunditz, "Improved Maximum-Torque-Per-Ampere Algorithm Accounting for Core Saturation, Cross-Coupling Effect, and Temperature for a PMSM Intended for Vehicular Applications," in *IEEE Transactions on Transportation Electrification*, vol. 2, no. 2, pp. 150-159, June 2016. doi: 10.1109/TTE.2016.2528505

XIII. Biographies

Antonino Di Gerlando received his MS degree in electrical engineering from the Politecnico di Milano, Italy, in 1981. Currently, he is a Full Professor at the Department of Energy at Politecnico di Milano. Fields of interest: design and modeling of electrical machines, converters and drive systems. He is a senior member of IEEE and a member of the Italian Association of the Electric and Electronic Engineers (AEI).

Giovanni Maria Foglia received his MS degree and the PhD in electrical engineering at Politecnico di Milano, Milano, Italy, in 1997 and 2000.
Currently, he is an Associate Professor at the Department of Energy at Politecnico di Milano, and his main field of interest is the analysis and design of PM electrical machines.

Roberto Perini (M'10) received his MS degree and the PhD in electrical engineering from the Politecnico di Milano, Milano, Italy.
Currently, he is an Associate Professor at the Department of Energy at Politecnico di Milano. His interests are in the design and modeling of electrical machines and power electronics.